Science of the Total Environment 634 (2018) 1315–1325

Contents lists available at ScienceDirect

Science of the Total Environment

journal homepage: www.elsevier.com/locate/scitotenv

Dynamic assessments of population exposure to urban greenspace using multi-source big data

Yimeng Song [a], Bo Huang [a,*], Jixuan Cai [a], Bin Chen [b]

[a] Department of Geography and Resource Management, The Chinese University of Kong Hong, Shatin, Hong Kong
[b] Department of Land, Air and Water Resources, University of California, Davis, CA 95616, USA

HIGHLIGHTS

- High-spatial-resolution images were used for urban greenspace extraction.
- City-level population exposure to urban greenspace was dynamically assessed.
- Neglecting human mobility led to erroneous results in exposure assessment.
- Diurnal and daily variations of exposure to urban greenspace were identified.

GRAPHICAL ABSTRACT

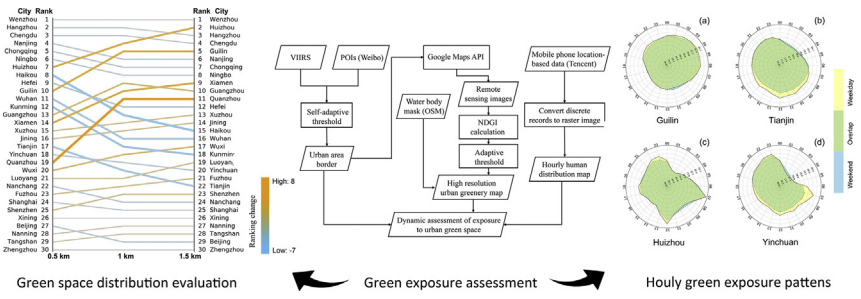

ARTICLE INFO

Article history:
Received 9 December 2017
Received in revised form 5 April 2018
Accepted 5 April 2018
Available online 18 April 2018

Editor: Simon Pollard

Keywords:
Urban greenspace
Human mobility
Dynamic assessment
Geo-spatial big data
Public health

ABSTRACT

A growing body of evidence has proven that urban greenspace is beneficial to improve people's physical and mental health. However, knowledge of population exposure to urban greenspace across different spatiotemporal scales remains unclear. Moreover, the majority of existing environmental assessments are unable to quantify how residents enjoy their ambient greenspace during their daily life. To deal with this challenge, we proposed a dynamic method to assess urban greenspace exposure with the integration of mobile-phone locating-request (MPL) data and high-spatial-resolution remote sensing images. This method was further applied to 30 major cities in China by assessing cities' dynamic greenspace exposure levels based on residents' surrounding areas with different buffer scales (0.5 km, 1 km, and 1.5 km). Results showed that regarding residents' 0.5-km surrounding environment, Wenzhou and Hangzhou were found to be with the greenest exposure experience, whereas Zhengzhou and Tangshan were the least ones. The obvious diurnal and daily variations of population exposure to their surrounding greenspace were also identified to be highly correlated with the distribution pattern of urban greenspace and the dynamics of human mobility. Compared with two common measurements of urban greenspace (green coverage rate and green area per capita), the developed method integrated the dynamics of population distribution and geographic locations of urban greenspace into the exposure assessment, thereby presenting a more reasonable way to assess population exposure to urban greenspace. Additionally, this dynamic framework could hold potential utilities in supporting urban planning studies and environmental health studies and advancing our understanding of the magnitude of population exposure to greenspace at different spatiotemporal scales.

1. Introduction

Urban greenery is one of the most important factors in the urban environment and considerably mitigates many urban problems, such as

* Corresponding author.
E-mail address: bohuang@cuhk.edu.hk. (B. Huang).

https://doi.org/10.1016/j.scitotenv.2018.04.061
0048-9697/

regulating urban climate and alleviating urban heat island effects (Andersson-Sköld et al., 2015), absorbing particle air pollutants (Janhäll, 2015), infiltrating storms (Livesley et al., 2016), and reducing noise levels (Van Renterghem and Botteldooren, 2016). Additionally, urban greenspace serves as the main places for residential activities and social interactions, contributing a lot to citizens in both physical and mental health. Previous studies have shown that as hotspots for citizens' physical activities, those large urban greenspaces (e.g., urban forests and parks) contribute indirectly to reducing risks of all-cause mortality and numerous chronic diseases (Wolch et al., 2014). Psychological well-being was also verified to correlate with green colors from urban greenspaces (Ernstson, 2013), since population exposure to greenery has widely proven to reduce stresses (Woo et al., 2009), and help self-recuperation and rejuvenation (Fuller et al., 2007).

Unprecedented rural-to-urban migrations have been witnessed in China over the past decades, leading to a huge rise in urban population from 191 million (1980) to 793 million (2016) (China, 2017), and the urban population is projected to reach 830 million by 2030 (Gong et al., 2012). Globally, the total population has been estimated to reach 10 billion by 2050, and 75% of them will live in urban regions (Giles-Corti et al., 2016). Thus, the urban environment is becoming critically important to the healthy cities and directly affecting every aspect of daily lives for urban residents. However, the rapid urbanization has greatly reshaped land cover and land use types, which dramatically changed urban green space in both quality and quantity. For example, a study of 90 Chinese major cities reported that more than 80% of the analyzed cities suffered a decline of urban green coverage at both old and new urban areas from 2000 to 2014 (Chen et al., 2017). Consequently, the distribution of urban greenspace is rarely even or equitable (Wolch et al., 2014). That is, the opportunities of exposure to greenery will be considerably different for citizens that live in different regions.

Green coverage rate (GCR, which is the greenspace area divided by a city's urban area as a percentage) and greenspace area per capita (GAC, which is the greenspace area divided by the urban population as m^2/capita) are the widely used indicators for assessing a city's green environment quality (Fuller and Gaston, 2009; Yang et al., 2014; Zhao et al., 2013). Although these indicators give an overall assessment of greenery levels for the entire study area, they are unable to reveal people's actual exposure to urban greenspace. Thus, some pioneering studies have been working on the reasonability of urban greenspaces' distribution and their service efficiency. For example, the assessment of population exposure to greenspace and its related epidemiological studies were conducted by means of questionnaire surveys and quantitative approaches such as GIS techniques and geospatial data. Questionnaire surveys and in-depth interviews can help researchers accurately know about interviewees' diurnal and daily green experience (Barbosa et al., 2007). However, their high expenses and limited samples barricade the data availability at large-scale studies (Chen et al., 2018). The integration of GIS techniques with geospatial data overcomes the limitation of spatial scales and sample sizes, thereby enabling it to quantify the geographic distribution and accessibility of urban greenspace from regional to global scales (Chen and Chang, 2015; Comber et al., 2008; Higgs et al., 2012). Nevertheless, these methods are still unable to fully estimate the actual time-varying exposure to greenspace, since the previous studies using population data (e.g., census data) always assumed that the population distribution is static without considering the spatiotemporal changes of residents' locations (Chen et al., 2018; Kwan, 2012), which inevitably lead to a biased assessment of population exposure to urban greenspaces.

In reality, people living in cities are constantly moving and rarely staying put in the same place all the time. Daily routines from working to education, shopping, exercise, and other activities will make people expose to different surroundings. Thus, how to combine human mobility into the context of greenery exposure assessments will be the key to better quantify the relationship between human and their changing surroundings across space-time scales. Fortunately, the rapid development of mobile Internet and the popularization of diverse applications (apps) with location-based services (LBS) on smartphones have generated huge amounts of human activity records, making it possible for researchers to access direct information of human geographical distribution (Liu et al., 2015). The high correlation between mobile-phone location-based records and spatiotemporal characteristics of human activities has also been verified in several studies (Dunkel, 2015; Gariazzo et al., 2016). Compared with the static data sources such as demographic data, the location-based geospatial big data are much better indicators to quantify the dynamic of population distribution with a finer spatiotemporal scale. Meanwhile, the increasing release of open data, such as Google Maps and OpenStreetMap (OSM) (Kitchin et al., 2017; See et al., 2016), provides further opportunities for us to describe and understand the surroundings of urban residents.

To addresses the abovementioned limitations of existing methods, by combining human mobility into environmental exposure assessment, we proposed a novel method to dynamically assess population exposure to urban greenspace with the integration of multi-source geospatial big data. Experimental tests with the developed method in 30 Chinese cities uncovered a better understanding of residents' diurnal and daily greenery exposure experiences and also revealed different facets of residents' greenery exposure among these cities with different physical and socio-economic characteristics. The remainder of this paper is organized as follows. Section 2 gives a brief description of the study area and the selected datasets. Sections 3 and 4 provide detail illustrations of the methods and results. We discuss the implications and main findings in Section 5 and offer our conclusions in Section 6.

2. Study area and data

2.1. Study area

Based on the city's size (area and population) and the availability of remote sensing imagery, thirty Chinese cities with population over 1.6 million (China, 2017) were selected as the experimental samples for the greenery exposure assessment in this study. They included four direct-controlled municipalities (Beijing, Shanghai, Tianjin, and Chongqing), thirteen provincial capitals (Zhengzhou, Xining, Nanchang, Yinchuan, Nanning, Kunming, Fuzhou, Wuhan, Nanjing, Hefei, Haikou, Guangzhou, and Chengdu), and thirteen others (Tangshan, Luoyang, Quanzhou, Shenzhen, Guilin, Wuxi, Xuzhou, Ningbo, Xiamen, Huizhou, Jining, Hangzhou, and Wenzhou).

To make a comprehensive evaluation of urban greenspace, we gathered several datasets (Table. S1 in Supplementary Materials) and provided the detailed information about them as below.

2.2. Nighttime light data

Nighttime light data from the Visible Infrared Imaging Radiometer Suite (VIIRS) with a 15 arc-second (~500 m) spatial resolution was used to identify the spatial extent of cities' urban areas. The nighttime light data (monthly composites) were obtained directly from the Earth Observation Group (EGO) of National Oceanic and Atmospheric Administration (NOAA) website (https://ngdc.noaa.gov/eog/), and any interference from stray light, lunar illumination, and cloud cover was filtered out. Specifically, 13 scenes covering the 30 cities from April 2015 to April 2016 were collected in this study. Pixel-based average composition images of the 13 scenes was then conducted for each city to reduce noise and recover bad values. Finally, the images were re-projected into the UTM projection with a 500-m spatial resolution.

2.3. High spatial resolution satellite data

Although the satellite data with moderate spatial resolutions such as Landsat have been widely used in vegetation extraction and urban greenspace detection (Chen et al., 2017; Fung and Siu, 2001; Zhou and

Wang, 2011), their spatial details may still over- or under-estimate the actual coverage of greenspaces (Qian et al., 2015). Such kind of biased magnitudes will be particularly large when small and fragmented greenspace exists, which is very common in high-density cities (Gariazzo et al., 2016). In contrast, satellite images such as QuickBird and Worldview from Google Earth/Maps offer an efficient and free-access proxy to extract urban greenspaces accurately (Pulighe and Lupia, 2016; Taylor and Lovell, 2012). In this study, we collected all high-spatial-resolution satellite images (~0.6 m) that are retrieved between 2014 and 2016 using the Google Static Maps application program interface (API, https://goo.gl/jY4HTc) for all selected cities. All images were further filtered by visual inspections to ensure that they were captured around summertime.

2.4. Mobile phone locating-request big data

Mobile-phone locating-request big data (MPL) were used to quantify spatiotemporal variabilities of residents' distribution by retrieving real-time locating-request records of location-based services (LBS) from mobile phone apps. The data used in this study were from Tencent (one of the largest Internet company in China), and the locating-request records were retrieved every 5 min with a spatial resolution of approximately 1.2 km. With the widespread use of Tencent apps (e.g., WeChat, QQ, Tencent Map) and Tencent's location-based services, the daily locating-request records were up to over 36 billion in 2016 (Tencent, 2016). Specifically, the dataset used in this study was collected between March 19 and November 21, 2016 using the Tencent API (http://heat.qq.com). The discrete locating-request records were first converted to raster images, and the generated time-resolved population distribution maps were then used to measure hourly and daily exposure to urban greenspace.

2.5. Other data

Administrative boundaries in the form of 1:4,000,000 maps were obtained from the National Fundamental Geographical Information System of China. These boundaries were used to separate adjacent cities and eliminate the blooming effects of nighttime light images, especially for coastal cities.

The LandScan Global Population dataset with a 1-km spatial resolution in 2015 was acquired for calculating the greenspace area per capita (GAC). This dataset was produced by the Oak Ridge National Laboratory using a multi-layered, dasymetric, spatial modeling approach with GIS and remote sensing techniques (Dobson et al., 2000).

Points of interest (POIs) have been widely used in urban studies (Cai et al., 2017; Hu et al., 2016; Zhang et al., 2017), as they represent locations with a series of information including function, location, and other geographic features. Here we used POIs in December 2015 from the Weibo social media platform through the open API (http://open.weibo.com/). All the POIs were categorized into nine groups (i.e., catering, retailing, automobile, accommodation, recreation, public facility, transportation, culture and media, others), and those highly relevant to human activities were selected and labeled as "urban area" based on these categories (Table S2 in Supplementary Materials). Finally, 300 thousand POIs (marked with urban area samples) were collected and used for extracting the urban area of each city.

3. Methods

Fig. 1 presents a flowchart outlining the methodology used in this study, including the following four main procedures. First, data preprocessing consisted of (i) selecting and labeling POIs data as urban area samples, (ii) averaging monthly nighttime light images, and (iii) converting discrete Tencent-based MPL data into raster images. Second, a self-adaptive method was applied to define each city's urban area using POIs and nighttime light images (VIIRS). Third, urban greenspace areas were extracted from fine-spatial-resolution satellite images. Finally, a dynamic assessment of population exposure to urban greenspace at different spatial scales was conducted.

3.1. Extraction of the urban area

The urban area was first extracted for all selected cities to ensure our focuses on the urbanized environment. Here we applied a self-developed adaptive approach to determine optimal thresholds for each city's urban area extraction by the integration of nighttime light imagery and POIs. First, nighttime light images were extracted with administrative boundaries for all the 30 cities. Second, for each selected city, by overlapping the POIs and nighttime light images, each P_i (POIs with urban area sample) would have a corresponding night-time-light intensity value (NIV) N_i. Taking Beijing for an instance (Fig. 2a), the majority of POIs' NIV ranged from 12 to 66 (Fig. 2b). To exclude potential biases such as negative values, null values and noises from NIVs, we assigned the cutting-off probability as 5% to refine NIVs of the POI samples, and the corresponding NIV was defined as the threshold for

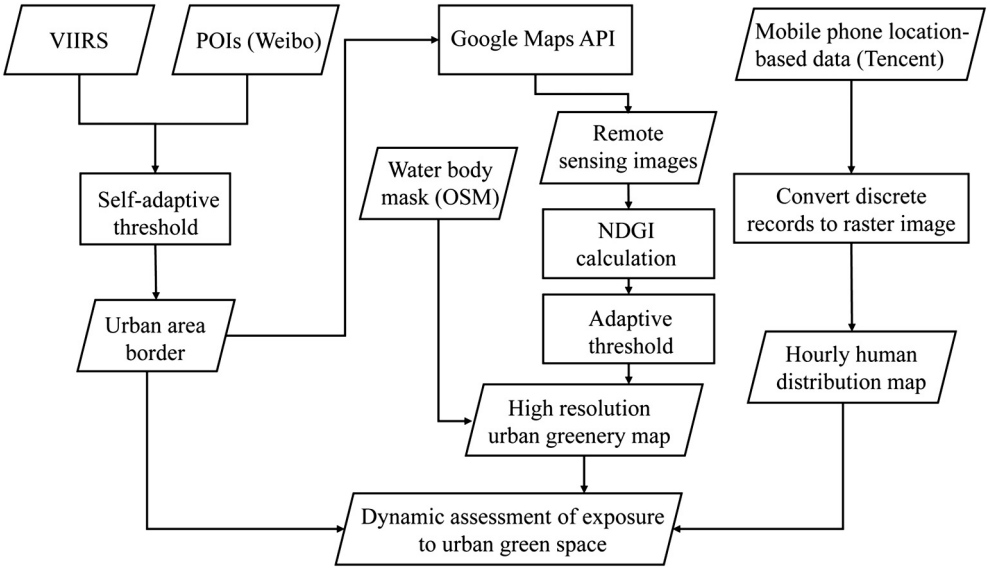

Fig. 1. Flowchart of the research methodology.

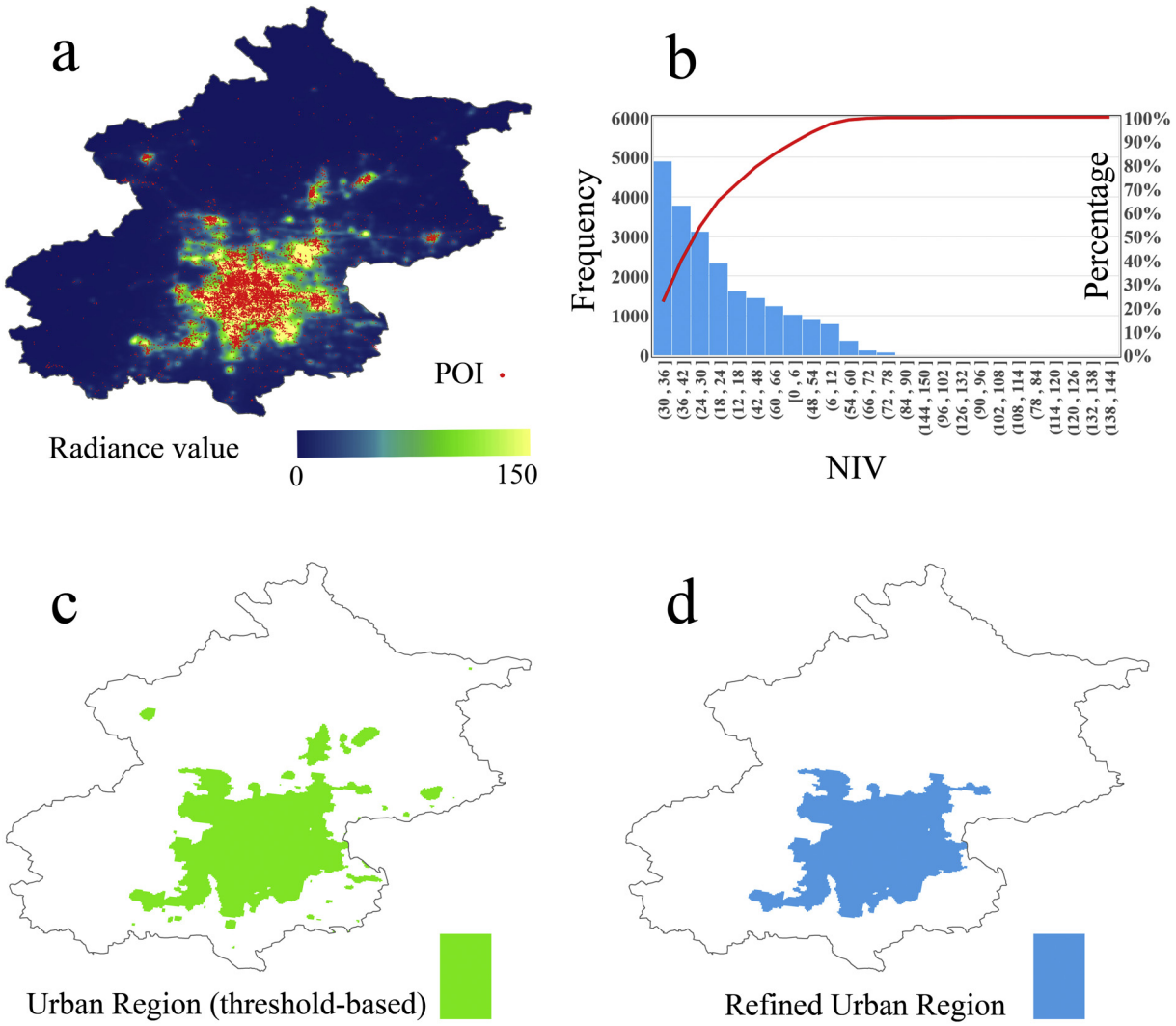

Fig. 2. Extraction of the urban area, taking Beijing for an instance. (a) Nighttime light image extracted with Beijing's administrative boundary. (b) The frequency and percentage of nighttime-light intensity value (NIV) extracted by points of interest (POI) samples in Beijing. (c) Urban region extracted by the adaptive NIV threshold. (d) The final refined urban area.

extracting urban areas. That is, pixels with NIVs equal to or larger than the threshold were regarded as urban areas (Fig. 2c). The final urban area for each city was refined by keeping the urban center and removing those spatially isolated pixels and small regions such as edge cities and satellite towns (Fig. 2d).

3.2. Extraction of urban greenspaces

Urban greenspaces involve all kinds of areas covered by green vegetation within the urban region (e.g., greenways, street trees, nature conservation areas, private backyards, community gardens, parks, sporting fields, etc.) (Wolch et al., 2014). With geographic boundaries of all selected cities, we accessed to the Google Maps tile-based images with an ~0.6-m spatial resolution at a zooming level of 18. All the selected tiles were then mosaicked and re-projected into the UTM projection system with a spatial resolution of 1 m. Due to the fact that the downloaded images from Google Maps are all R-G-B composition with digital values ranging from 0 to 255, we are unable to extract remote-sensing indicators such as Normalized Difference Vegetation Index (NDVI) and Enhanced Vegetation Index (EVI) that require near-infrared bands. However, since our study areas are the context of urban regions without extensive farmlands, we can regard all green pixels identified from Google Map images as parts of urban greenspaces. To eliminate potential noises from aquatic plants in water bodies, the water body layer from OpenStreetMap was used to mask out the Google Map images. Finally, we used the Normalized Difference Greenness Index (NDGI) (Uto et al., 2008) to measure the greenness of each pixel as

$$\mathrm{NDGI} = \frac{G - R}{G + R} \quad (1)$$

where R, and G are digital values of red and green bands, respectively. With lots of trial-and-error experiments in this study, the urban greenspace pixels were defined as the NDGI value greater than 0.2 and the digital value of the blue band lower than 200. An example of extracting urban greenspaces is presented in Fig. 3. The average accuracy of the obtained results was 85.14% (ranging from 79.52% to 91.20%). More detail information about the validation process can be found in Supplementary Materials (accuracy validation of greenspace extraction).

3.3. Dynamic green exposure assessment

Since the location of an individual is temporally varied, to objectively reflect population exposure to ambient greenspace environment across

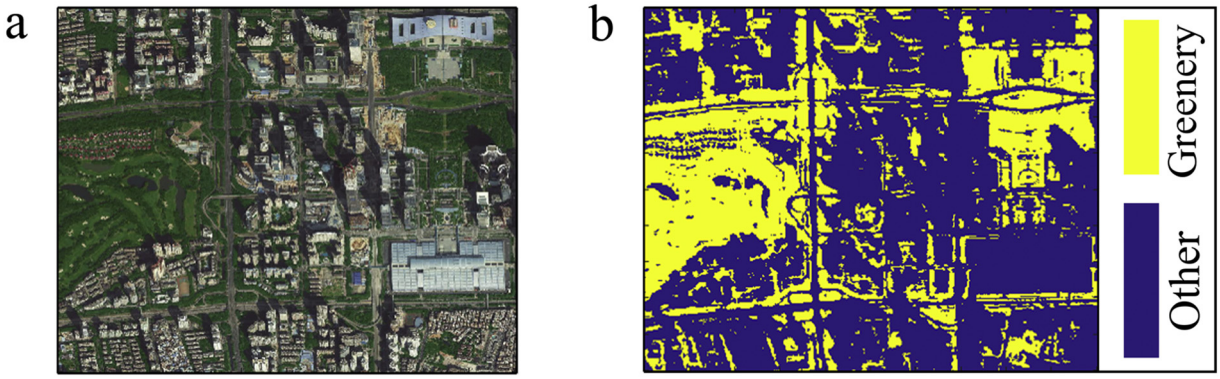

Fig. 3. Urban greenspace extraction. a. High-resolution remote sensing image collected from Google Maps. b. Extracted greenspaces based on the Normalized Difference Greenness Index (NDGI) and blue band.

different temporal scales, a model for dynamically assessing greenery exposure, termed "green exposure" is defined as Eq. (2)

$$GE = \frac{\sum_{i=1}^{n} G_i}{n} \tag{2}$$

where G_i denotes the green level of the ith individual's surrounding environment, n is the total population within the study area, and GE is the average green exposure of the targeted study area (e.g., the urban area of a city).

In this study, the MPL data was used as an indicator to delineate the spatiotemporal pattern of population distribution since the time-series gridded MPL data could represent the relative population dynamics. By incorporating the real-time dynamics of pixel-based population distribution into the green exposure assessment, we further modified the model in Eq. (2) in a population-weighted manner. Thus, the green exposure could be calculated as

$$GE = \frac{\sum_{i=1}^{n} (p_i \times G_i)}{\sum_{i=1}^{n} p_i} \tag{3}$$

where p_i is the relative amount of population in the ith grid, and G_i is the green level of the area around the ith grid. Specifically, we used the green coverage rate to evaluate the green level of a region. GE denotes the green exposure (population-weighted average greenery coverage) of the target study area.

To calculate the green coverage rate in the surrounding areas, a center point for each grid was first defined with the assumption that all of the locating-request records (representing people's real-time locations) within the grid (1 km * 1 km) were centered with this point. Buffers with different distances were then built from the center point to define different surrounding areas. In this study, three buffer scales regarding the green exposure were assessed with distances from 0.5 km to 1 km, and 1.5 km away from the center point of each grid. Specifically, green exposure with the buffer scale of 0.5 km was used to evaluate population exposure to immediate surrounding greenspaces which was shown to have the function of improving the microenvironment and exerting positive effects on mental health (Bowler et al., 2010). The larger 1.5-km buffer scale was used to account for greenspaces nearby and within a certain distance, since greenspaces within a certain distance can also contribute to purifying local air quality and relieving local heat island effects (Mitchell et al., 2011). The 1-km buffer scale was selected as the transitive level to understand the change pattern of a city's green exposure from small to large scales. As it was hard to provide any information about the individuals' precise positions in each pixel (e.g., indoor-outdoor ratio), the defined green exposure in this study represented as the maximum potential exposure level to the surrounding greenspaces.

With the high-spatial-resolution greenspace mapping and the real-time dynamics of MPL-based dynamic population distribution, we can estimate the magnitude of population exposure to their ambient greenspaces based on Eq. (3) with different updating frequencies from 5 min to one day, one month or even one year. In this study, to reduce computational costs, we first aggregated the 5-min MPL data into hourly MPL data for each city and aimed to give a general assessment of hourly population exposure to surrounding greenspaces in the 30 selected cities.

3.4. Evaluation of urban greenspace distribution

To quantify the difference in greenspace distributions among the 30 selected cities, a sensitivity analysis was conducted by comparing each city's rankings in the magnitude of green exposure across different buffer scales. Generally, if a city has relatively stable rankings in different buffer scales (i.e., 0.5 km, 1 km, and 1.5 km), it means that the city is less sensitive to the change of buffer scales in terms of green exposure, otherwise, the targeted city will be more sensitive to the variation of buffer scales. Ideally, if a city has high rankings and a low sensitivity across different buffer scales, it means that the distribution of urban greenspaces in this city is quite reasonable and the total green coverage is with a relatively high level. For those have high sensitivity, cities with high ranking in a smaller buffer scale is better than those having high ranking in a larger buffer scale, since the former cities put most of the limited greenspace close to their citizens.

3.5. Comparison of exposure assessment between the dynamic and static methods

In order to investigate whether the dynamic model dose make a different in the assessment of population exposure to urban greenspace, we intuitively compared the rankings of the results from the MPL-based dynamic method and the commonly used static method for all the selected cities. The rankings of dynamic-based results were received based on the average of all the hourly green exposure from March 19 and November 21, 2016. For the evaluation of urban greenspace environment using the static method, we calculated green coverage rate and greenspace area per capita with the extracted greenspace distribution map, the urban region, and LandScan Global Population dataset for each city. It should be noted that the total population of each city was derived by aggregating the pixel-based population of LandScan within the newly defined urban area for the calculation of greenspace area per capita.

4. Results

4.1. Estimation of urban area and urban greenspaces

The urban areas of all cities were extracted by the integration of nighttime light images and POIs, while the urban greenspaces were

extracted from high-spatial-resolution images from Google Maps. Quantitatively, Shanghai (4373.10 km^2) and Beijing (3399.96 km^2) were two cities with the largest urban area, and Xining (188.44 km^2) was with the smallest urban area. Regarding the green coverage rate in the extracted urban region, the three cities with the highest green coverage rate were Chengdu, Wenzhou, and Guangzhou, whereas the lowest was Zhengzhou (Fig. 4). The total average green coverage rate for all the 30 cities was 36.41% (95% CI: 22.73%–49.20%).

4.2. Average green exposure

By taking the dynamics of population distribution into consideration, the hourly green exposures in three buffer scales were received (Fig. 5), from March 19 and November 21, 2016. Here we take the 0.5-km buffer scale for an example. As the whisker plot showed in Fig. 5, Chengdu, Wenzhou, and Hangzhou were the top three cities with highest green exposure in 0.5-km buffer scale, where residents could enjoy more greenspace than other cities within their 0.5-km surrounding context. In contrast, Zhengzhou, Tangshan, and Nanning were the lowest ones. Additionally, the green exposures of all the cities witnessed an upward trend along with the increasing buffer scales (Fig. 5), because a lager buffer size would gradually include more greenspaces in remote regions (e.g., parks, public spaces, grass land or forest land). Meanwhile, an obvious variability of hourly green exposure was identified from the whisker plot in Fig. 5 that the quartile values of some cities were found to be up to ±25% wider than their median values, which demonstrated that the human mobility contributed significantly to their varied surrounding greenspace environment.

4.3. Difference of greenspace distribution across the selected cities

As shown in Fig. 6, cities with relatively stable rankings in different buffer scales were assigned with a low sensitivity, otherwise, their sensitivity would be high. Based on the magnitude of green exposure and its corresponding sensitivity, here we categorized them into four groups. (1) The first group includes cities with low sensitivity & high green exposure in all buffer scales (LS-HG), such as Wenzhou, Hangzhou, and Chengdu, indicating the greenspace distribution in these cities is reasonable and amount of greenspace is also large, and residents in these cities are able to enjoy more greenspace than those in other cities. (2) The second group includes cities with low sensitivity & low green exposure in all buffer scales (LS-LG), such as Beijing, Nanjing, Tangshan and Zhengzhou. Compared with other groups of cities, residents in these cities are limited to experiencing enough greenspace during their daily life. (3) The third group includes cities with high sensitivity & low green exposure in smaller (0.5 km) buffer scale (HS-LG_s). Cities in this group have low rankings in a smaller buffer scale but better rankings in a larger buffer scale. For example, the cities such as Huizhou, Guilin, Quanzhou, and Wuxi, their rankings are becoming better with a larger buffer scale, which means that the majority of greenspaces are far from residents rather than being nearby. (4) The fourth group includes cities with high sensitivity & high green exposure in smaller (0.5 km) buffer scale (HS-HG_s). This group of cities has better performance in smaller buffer scales but poor performance in larger buffer scales (e.g., Haikou, Wuhan, Kunming, and Tianjin), which means that the distribution of urban greenspaces is friendly. Despite of the limited amount of greenspaces, the majority of them are distributed near the residents so that people can immediately and easily benefit from them.

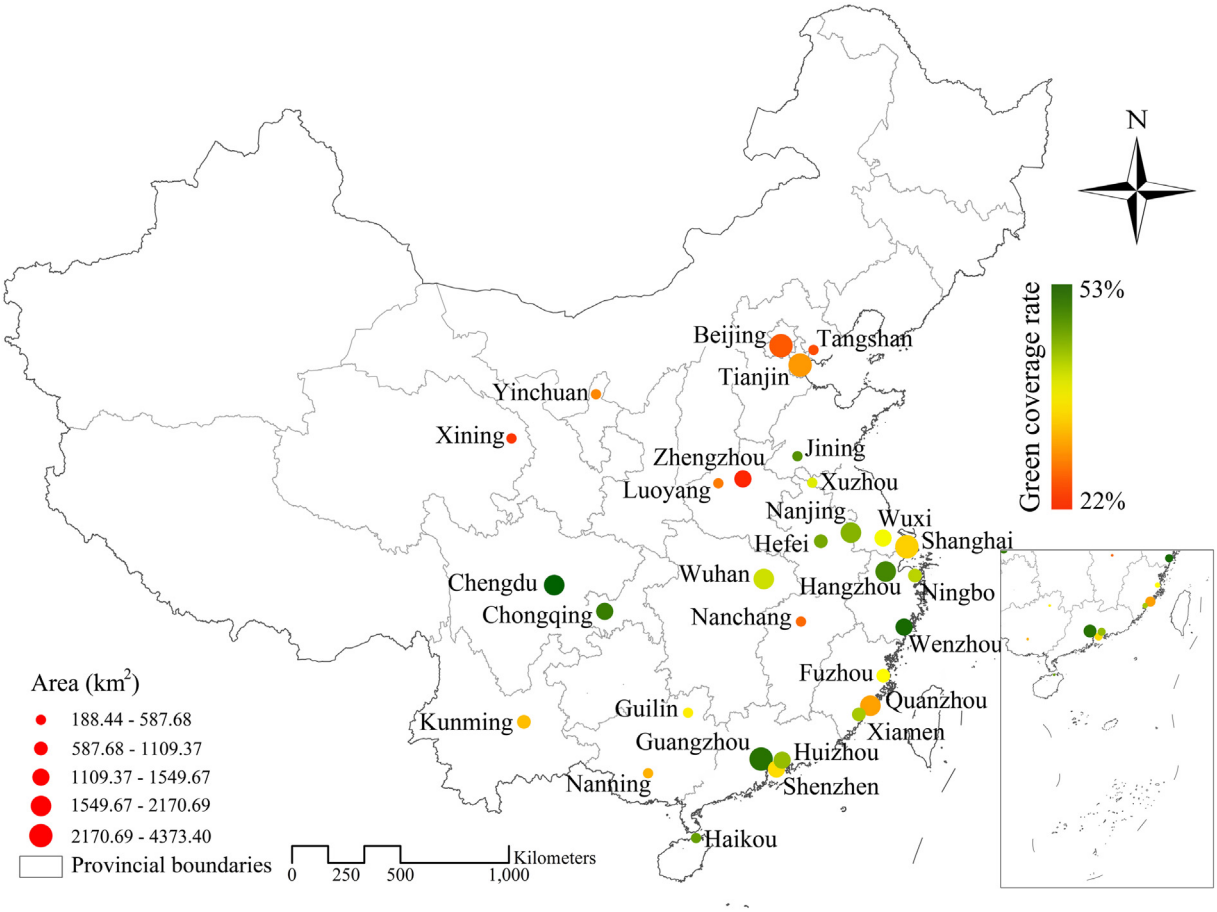

Fig. 4. Urban areas and green coverage rate of all the selected cities. The circle size denotes the total areas of the extracted urban center region for each city. The stretched colors from red to green denote varied magnitudes of green coverage rate for each city.

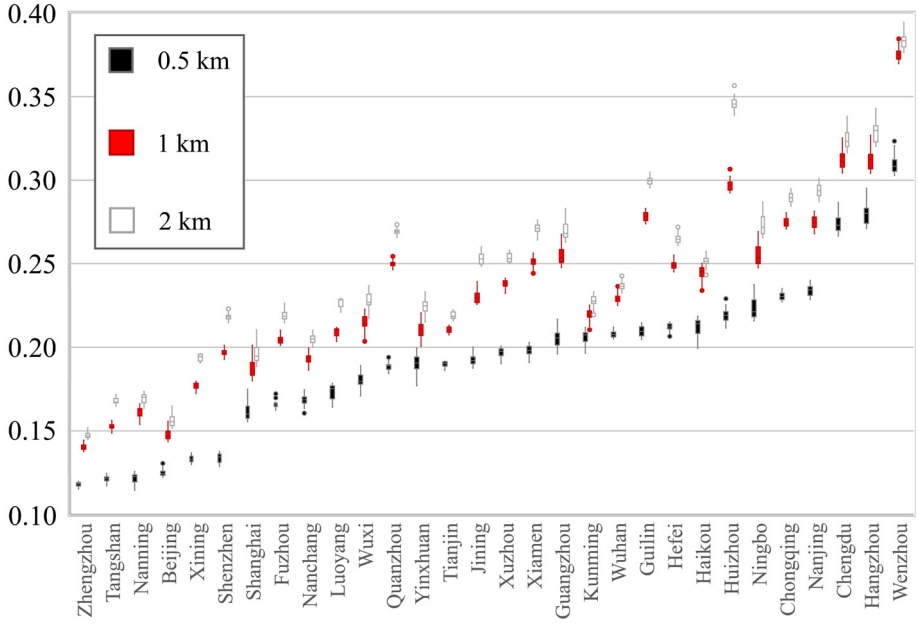

Fig. 5. Whisker plot of hourly green exposure in 0.5-km, 1-km and 2-km buffer scales.

4.4. Dynamic change of green exposure

Based on the hourly population distribution map, we assessed the 30 cities' dynamic green exposure changes in 0.5-km buffer size for weekdays and weekends, respectively. All the results were presented in the form of rose diagrams in Fig. S1 (Supplementary Materials). For the purpose of uncovering different exposure patterns across temporal scales, we selected four cities with representative green exposure patterns, including Guilin, Tianjin, Huizhou, and Yinchuan, as shown in Fig. 7. For convenience, we used workplaces and schools to represent the places where people are in the daytime and used home and residences to represent the places where people are in the nighttime. (i) As Fig. 7a shown, the magnitude of green exposure in 0.5-km buffer scale between 24:00 and 06:00 was obviously greater than that between 09:00 to 18:00. This pattern illustrated that people living in cities such as Guiyang enjoyed more greenery during nighttime (when most

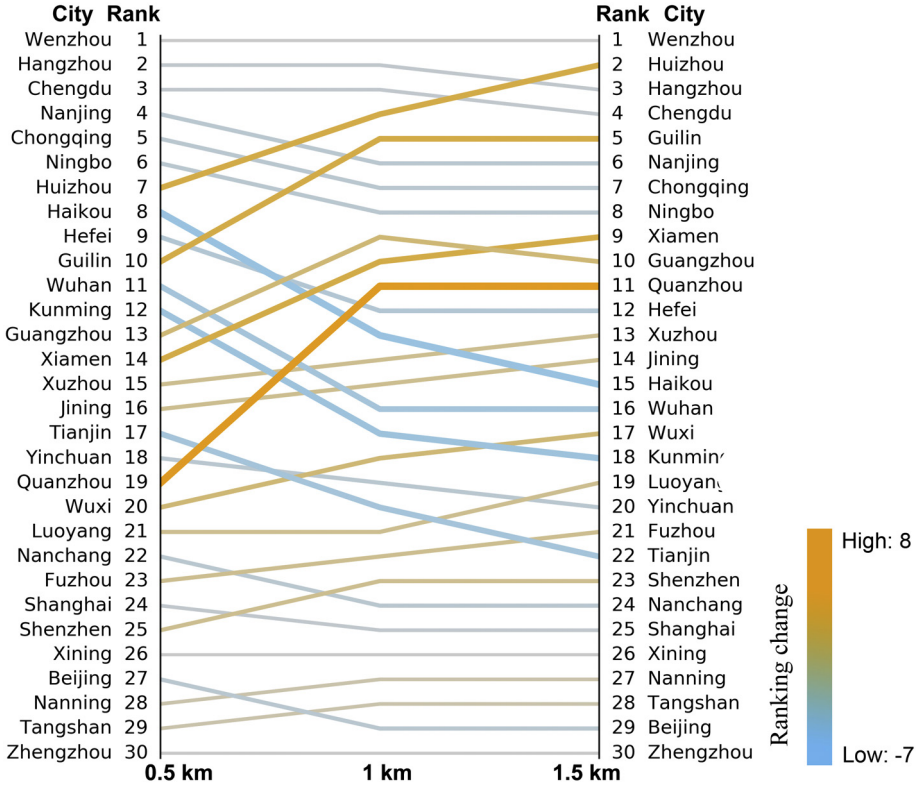

Fig. 6. Inter-city ranking and sensitivity analysis for 30 cities' green exposure with three different buffer scales. The thickness of line indicates the absolute value of the ranking change ($Rank_{1.5km}$–$Rank_{0.5km}$): the thicker the larger. The color of line denotes positive (orange) or negative (blue) values.

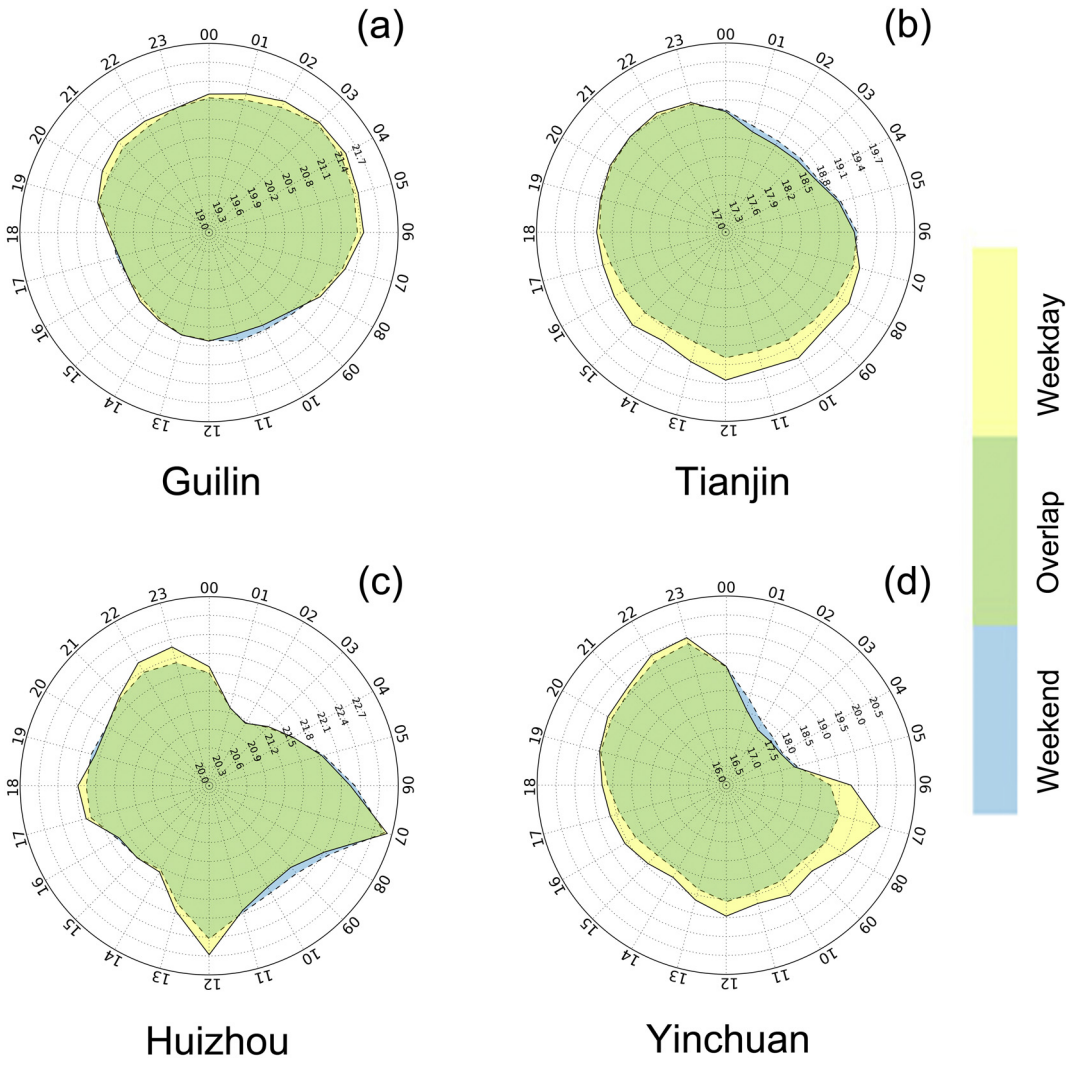

Fig. 7. Patterns of hourly green exposure in 0.5-km buffer scale for the cities Guilin, Tianjin, Huizhou, and Yinchuan. Regions in yellow are the green exposure on weekdays, regions in blue are that on weekends, and regions in green are the overlaps.

people were at home) than daytime (when most people were at their workplaces or schools). (ii) However, cities like Tianjin (Fig. 7b) were in the opposite situation, where the green coverage within people's surrounding 0.5 km area during nighttime was less than that during daytime. (iii) The third pattern is quite different from the first two, as the hourly green exposure changed drastically during the day. People in cities such as Huizhou (Fig. 7c) enjoyed obviously greener environment at around 07:00 and 12:00. Typically, during these two periods, most people in China are on the way to work or school (around 07:00) and go out for lunch or other non-work activities (around 12:00), which change their locations from indoor to outdoor. Therefore, in the cities like Huizhou, comparing with the relatively less greenspace surrounding citizens' residences or workplaces (or schools), more green vegetation was located along the streets, roads and other places where people were during these two periods. (iv) The exposure pattern in cities like Yinchuan (Fig. 7d) appears to be a combination of the patterns of Tianjin (Fig. 7b) and Huizhou (Fig. 7c), as more green vegetation was located around people's work spaces than around their residences, and abrupt changes can also be found at around 07:00 and 12:00.

4.5. Difference of green exposure between weekdays and weekends

As shown in Fig. 7 and Fig. S1, the diurnal variations of green exposure on weekdays and weekends are in similar patterns for most cities. However, they do exhibit some differences, for example in Yinchuan (Fig. 7d), the average green exposure on weekdays at around 07:00 was much higher than that on weekends. One possible reason is that people need to collectively move from their homes to their workplaces (or schools) in the morning on weekdays, whereas the majority do not commute over the weekends. Thus, we calculated the change rate of green exposure in 0.5-km buffer scale using Eq. (4) to describe the difference between weekdays and weekends.

$$P = \frac{AE_d - AE_e}{AE_d} \times 100\% \tag{4}$$

where P is the change rate of green exposure between weekdays and weekends, AE_d is the city-scale average green exposure on weekdays, and AE_e is the city-scale average green exposure on weekends.

As shown in Fig. 8, residents in nine of the thirty cities enjoy fewer greenspaces on weekdays than weekends ($AE_d < AE_e$), and Shanghai has the largest change rate of green exposure (1.67%). In contrast, residents in the other 21 cities are exposed to a better greenspace on weekdays than weekends ($AE_d > AE_e$), and the city exhibiting the largest difference was Nanchang (1.47%).

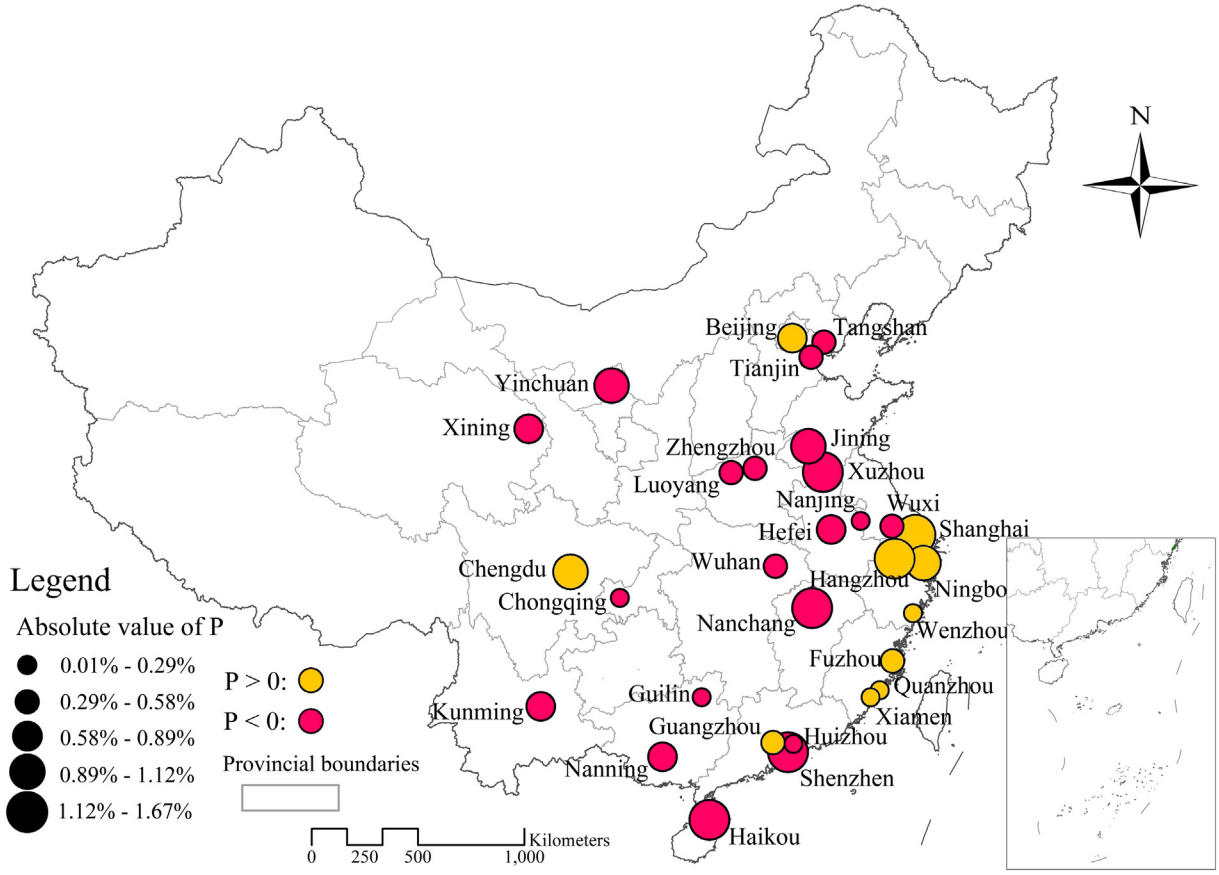

Fig. 8. Change rate of city-scale green exposure in 0.5-km buffer scale between weekdays and weekends.

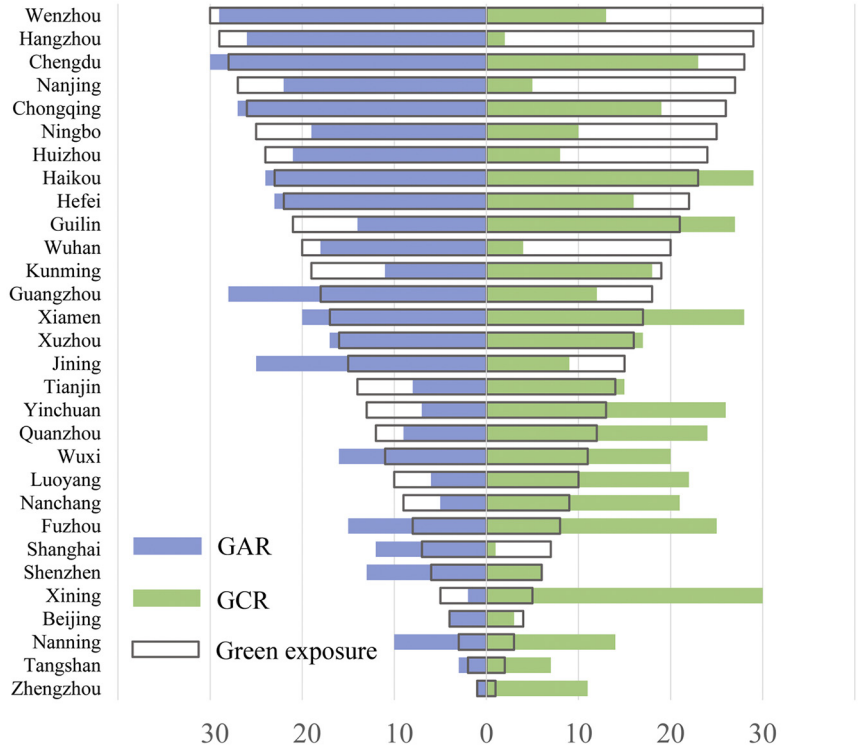

Fig. 9. Rankings of all 30 cities in terms of green area per capita (GAC), green coverage rate (GCR), and green exposure. The criterion differentiates the magnitude of green levels from greenest (30) to least green (1).

4.6. Comparison of different exposure assessment methods

The 30 cities' rankings on two indexes (green coverage rate and greenspace area per capita) as well as the rankings based on the dynamic green exposure were shown in Fig. 9. Each box plot displays the ranking of the city in the corresponding index, and the city with the highest green level was marked as 30 (e.g., Chengdu in green coverage rate) and the city with the lowest green level was marked as 1 (e.g., Zhengzhou in green coverage rate). It can be obviously identified that the rankings of most cities in terms of these three indexes are different. Taking Wuxi for an example, both its green coverage rate and greenspace area per capita are relative plausible, however, by considering the dynamics of population distribution into the assessment of population exposure to greenspace, results show that the residents' surrounding greenspace environment is not satisfied. Meanwhile, cities such as Wuhan has an opposite situation that even the city's overall green level in terms of green coverage rate and greenspace area per capita is not very high, but the majority of greenspaces are distributed nearby residents.

5. Discussion

In this study, by combining high-spatial-resolution remote sensing images from Google Maps and mobile-phone locating-request (MPL) data from Tencent, a novel model for dynamically assessing population exposure to urban greenspace was proposed and applied in 30 Chinese cities. Different from traditional methods of evaluating urban greenspace in terms of green area per capita and green coverage rate, or the static green exposure assessments based on census-based population data, the developed model well considered the spatiotemporal variability of population distribution and the accurate extraction of urban greenspaces, thereby contributing to a better assessment of population exposure to urban greenspace. The potential highlights of this model can be concluded as follows. First, given that the commonly used Landsat series (30 m) and MODIS 250–1000 m) data are still unable to capture sub-pixel complex urban environment accurately, especially for the highly urbanized areas, the high-spatial-resolution remote sensing images (0.5–1 m) are used in this study for extracting urban greenspace and deriving greenspace distribution maps with fine spatial details. Second, the human mobility is considered in the construction of the assessment model. Previous studies regarding the assessment of green exposure always used the census data based on the assumption that the population distribution is stationary. However, in reality, people will be in different places and experience different greenspace environment across different times. Thus, the mobile-phone locating-request (MPL) big data are used in this study to quantify dynamic changes of people's surrounding greenspace. The combination of high-spatial-resolution greenspace distribution maps and the real-time dynamics of population distribution will surely provide us more information about population exposure to different greenspaces during their daily life.

The temporal variation of green exposure reveals the shift of people's surrounding greenspace environment, which is mainly determined by the characteristics of greenspace distribution in urban areas. For example, the cities with a relatively higher magnitude of green exposure in the night always have better greenspaces for residential places. In contrast, cities with a higher magnitude of green exposure in the daytime will have better greenspaces for workplaces. Recently, more cities have been planting green vegetation along the streets and in public spaces, and such kind of efforts will contribute much to increasing the magnitude of green exposure when people are walking and commuting outside. In addition, the uncovered difference of green exposure between weekdays and weekends in this study results from the changes of people's commuting patterns and surrounding greenspace environment between these two periods.

The comparison of cities' rankings derived from the dynamic or static methods also supports our argument that ignoring human mobility may lead to biased assessment of population exposure to urban greenspace. The shortcomings of those static-based assessments have already been discussed in previous researches on environmental health/exposure, which are grouped as part of the uncertain geographic context problem (Kwan, 2012). That is, research conclusions about the effects of environmental influences on a person's health are sensitive to different delineations of the geographic and temporal contexts used to derive the relevant environmental variables. This issue can be found in the studies that use datasets with very low spatiotemporal resolution or aggregated over large regions (e.g., census tracts) that do not necessarily reflect individuals' travel trajectories or the dynamic change of population distributions, thereby limiting the ability to collect the actual ambient environment of people during their lives (Kwan, 2012; Park and Kwan, 2017). Therefore, the developed method for dynamic assessments of population exposure to green exposure in this paper provides an alternative to solve the uncertain geographic context problem and advance our understanding of the interaction between environment, human being, and public health.

Meanwhile, some potential concerns about the implementation of our methods should be addressed. First, geospatial big data (e.g., mobile phone location data, social media check-in records) are non-representative, they may omit some population groups of society such as children, the elderly, and the poor, who are less-frequent active users (Chen et al., 2018; Zagheni and Weber, 2015). However, such kind of big data are still good indicators for delineating real-time population distribution from local to regional scales. Second, the extraction of urban greenspace was conducted based on an empirical threshold method, which may limit the accuracy of greenspace distribution mapping to some extent. Therefore, how to integrate other data resources and methods to better map the high-spatial-resolution greenspace distribution will be our future work.

6. Conclusion

With the integration of multi-source geospatial big data, this study sought to propose a dynamic model of assessing population exposure to their surrounding greenspace environment, thereby providing a better way to understand how people expose to their ambient greenspace environment across different spatial-temporal scales. Experimental tests with 30 major cities in China revealed obvious diurnal and daily variations of population exposure to their surrounding greenspaces with different buffer scales, and the distribution pattern of urban greenspaces and the magnitude of green exposure were also varied across different cities. Compared with the static methods, the developed method uncovered a more reasonable assessment of green exposure by taking the urban greenspace patterns and the spatiotemporal variabilities of population distribution into consideration. This dynamic framework could hold potential utilities in supporting urban planning studies such as assessing the reasonability of urban greenspace distribution, adjusting the allocations of greenspaces and advancing our understanding of the magnitude of population exposure to greenspace at different spatiotemporal scales. Additionally, these methods and findings may contribute to building quantitative relationship between green exposure and related public health issues.

Acknowledgement

The authors thank Tencent Inc. for making the mobile-phone locating-request big data publicly available and Google Inc. for making the high-spatial-resolution satellite imagery publicly available. This work was supported by a project funded by the China Postdoctoral Science Foundation (2017M620739). The authors also thank anonymous reviewers and editors for providing valuable suggestions and comments, which have greatly improved this manuscript.

Appendix A. Supplementary data

Supplementary data to this article can be found online at https://doi.org/10.1016/j.scitotenv.2018.04.061.

References

Andersson-Sköld, Y., Thorsson, S., Rayner, D., Lindberg, F., Janhäll, S., Jonsson, A., Moback, U., Bergman, R., Granberg, M., 2015. An integrated method for assessing climate-related risks and adaptation alternatives in urban areas. Clim. Risk Manag. 7, 31–50.

Barbosa, O., Tratalos, J.A., Armsworth, P.R., Davies, R.G., Fuller, R.A., Johnson, P., Gaston, K.J., 2007. Who benefits from access to green space? A case study from Sheffield, UK. Landsc. Urban Plan. 83, 187–195.

Bowler, D.E., Buyung-Ali, L., Knight, T.M., Pullin, A.S., 2010. Urban greening to cool towns and cities: a systematic review of the empirical evidence. Landsc. Urban Plan. 97, 147–155.

Cai, J., Huang, B., Song, Y., 2017. Using multi-source geospatial big data to identify the structure of polycentric cities. Remote Sens. Environ. 202, 210–221.

Chen, J., Chang, Z., 2015. Rethinking urban green space accessibility: evaluating and optimizing public transportation system through social network analysis in megacities. Landsc. Urban Plan. 150–159.

Chen, B., Nie, Z., Chen, Z., Xu, B., 2017. Quantitative estimation of 21st-century urban greenspace changes in Chinese populous cities. Sci. Total Environ. 609, 956–965.

Chen, B., Song, Y., Jiang, T., Chen, Z., Huang, B., Xu, B., 2018. Real-time estimation of population exposure to PM2.5 using mobile-and station-based big data. Int. J. Environ. Res. Public Health 15, 573.

China, N., 2017. Statistical Communiqué of the People's Republic of China on the 2016 National Economic and Social Development. National Bureau of Statistics of China, Beijing.

Comber, A., Brunsdon, C., Green, E., 2008. Using a GIS-based network analysis to determine urban greenspace accessibility for different ethnic and religious groups. Landsc. Urban Plan. 86, 103–114.

Dobson, J.E., Bright, E.A., Coleman, P.R., Durfee, R.C., Worley, B.A., 2000. LandScan: a global population database for estimating populations at risk. Photogramm. Eng. Remote. Sens. 66, 849–857.

Dunkel, A., 2015. Visualizing the perceived environment using crowdsourced photo geodata. Landsc. Urban Plan. 142, 173–186.

Ernstson, H., 2013. The social production of ecosystem services: a framework for studying environmental justice and ecological complexity in urbanized landscapes. Landsc. Urban Plan. 109, 7–17.

Fuller, R.A., Gaston, K.J., 2009. The scaling of green space coverage in European cities. Biol. Lett. 5, 352–355.

Fuller, R.A., Irvine, K.N., Devine-Wright, P., Warren, P.H., Gaston, K.J., 2007. Psychological benefits of greenspace increase with biodiversity. Biol. Lett. 3, 390–394.

Fung, T., Siu, W.-L., 2001. A study of green space and its changes in Hong Kong using NDVI. Geogr. Environ. Model. 5, 111–122.

Gariazzo, C., Pelliccioni, A., Bolignano, A., 2016. A dynamic urban air pollution population exposure assessment study using model and population density data derived by mobile phone traffic. Atmos. Environ. 131, 289–300.

Giles-Corti, B., Vernez-Moudon, A., Reis, R., Turrell, G., Dannenberg, A.L., Badland, H., Foster, S., Lowe, M., Sallis, J.F., Stevenson, M., 2016. City planning and population health: a global challenge. Lancet 388, 2912–2924.

Gong, P., Liang, S., Carlton, E.J., Jiang, Q., Wu, J., Wang, L., Remais, J.V., 2012. Urbanisation and health in China. Lancet 379, 843–852.

Higgs, G., Fry, R., Langford, M., 2012. Investigating the implications of using alternative GIS-based techniques to measure accessibility to green space. Environ. Plann. B Plann. Des. 39, 326–343.

Hu, T., Yang, J., Li, X., Gong, P., 2016. Mapping urban land use by using landsat images and open social data. Remote Sens. 8, 151.

Janhäll, S., 2015. Review on urban vegetation and particle air pollution–deposition and dispersion. Atmos. Environ. 105, 130–137.

Kitchin, R., Lauriault, T.P., Wilson, M.W., 2017. Understanding Spatial Media. Sage.

Kwan, M.-P., 2012. The uncertain geographic context problem. Ann. Assoc. Am. Geogr. 102, 958–968.

Liu, Y., Liu, X., Gao, S., Gong, L., Kang, C., Zhi, Y., Chi, G., Shi, L., 2015. Social sensing: a new approach to understanding our socioeconomic environments. Ann. Assoc. Am. Geogr. 105, 512–530.

Livesley, S., McPherson, E., Calfapietra, C., 2016. The urban forest and ecosystem services: impacts on urban water, heat, and pollution cycles at the tree, street, and city scale. J. Environ. Qual. 45, 119–124.

Mitchell, R., Astell-Burt, T., Richardson, E.A., 2011. A comparison of green space indicators for epidemiological research. J. Epidemiol. Community Health 2010, 119172.

Park, Y.M., Kwan, M.-P., 2017. Individual exposure estimates may be erroneous when spatiotemporal variability of air pollution and human mobility are ignored. Health Place 43, 85–94.

Pulighe, G., Lupia, F., 2016. Mapping spatial patterns of urban agriculture in Rome (Italy) using Google Earth and web-mapping services. Land Use Policy 59, 49–58.

Qian, Y., Zhou, W., Yu, W., Pickett, S.T., 2015. Quantifying spatiotemporal pattern of urban greenspace: new insights from high resolution data. Landsc. Ecol. 30, 1165–1173.

See, L., Mooney, P., Foody, G., Bastin, L., Comber, A., Estima, J., Fritz, S., Kerle, N., Jiang, B., Laakso, M., 2016. Crowdsourcing, citizen science or volunteered geographic information? The current state of crowdsourced geographic information. ISPRS Int. J. Geo-Inf. 5, 55.

Taylor, J.R., Lovell, S.T., 2012. Mapping public and private spaces of urban agriculture in Chicago through the analysis of high-resolution aerial images in Google Earth. Landsc. Urban Plan. 108, 57–70.

Tencent, 2016. Tencent Annual Report. Tencent, Shenzhen, China, p. 2016.

Uto, K., Takabayashi, Y., Kosugi, Y., Ogata, T., 2008. Hyperspectral analysis of Japanese Oak wilt to determine normalized wilt index. Geoscience and Remote Sensing Symposium, 2008. IGARSS 2008. IEEE International. IEEE, pp. II-295–II-298.

Van Renterghem, T., Botteldooren, D., 2016. View on outdoor vegetation reduces noise annoyance for dwellers near busy roads. Landsc. Urban Plan. 148, 203–215.

Wolch, J.R., Byrne, J., Newell, J.P., 2014. Urban green space, public health, and environmental justice: the challenge of making cities 'just green enough'. Landsc. Urban Plan. 125, 234–244.

Woo, J., Tang, N., Suen, E., Leung, J., Wong, M., 2009. Green space, psychological restoration, and telomere length. Lancet 373, 299–300.

Yang, J., Huang, C., Zhang, Z., Wang, L., 2014. The temporal trend of urban green coverage in major Chinese cities between 1990 and 2010. Urban For. Urban Green. 13, 19–27.

Zagheni, E., Weber, I., 2015. Demographic research with non-representative internet data. Int. J. Manpow. 36, 13–25.

Zhang, X., Du, S., Wang, Q., 2017. Hierarchical semantic cognition for urban functional zones with VHR satellite images and POI data. ISPRS J. Photogramm. Remote Sens. 132, 170–184.

Zhao, J., Chen, S., Jiang, B., Ren, Y., Wang, H., Vause, J., Yu, H., 2013. Temporal trend of green space coverage in China and its relationship with urbanization over the last two decades. Sci. Total Environ. 442, 455–465.

Zhou, X., Wang, Y.-C., 2011. Spatial–temporal dynamics of urban green space in response to rapid urbanization and greening policies. Landsc. Urban Plan. 100, 268–277.